Neural coding in a single sensory neuron controlling opposite seeking behaviors in *Caenorhabditis elegans*

Atsushi Kuhara, Noriyuki Ohnishi, Tomoyasu Shimowada & Ikue Mori

Supplementary Information

Supplementary Figures S1-S5

Supplementary Note 1

Supplementary References

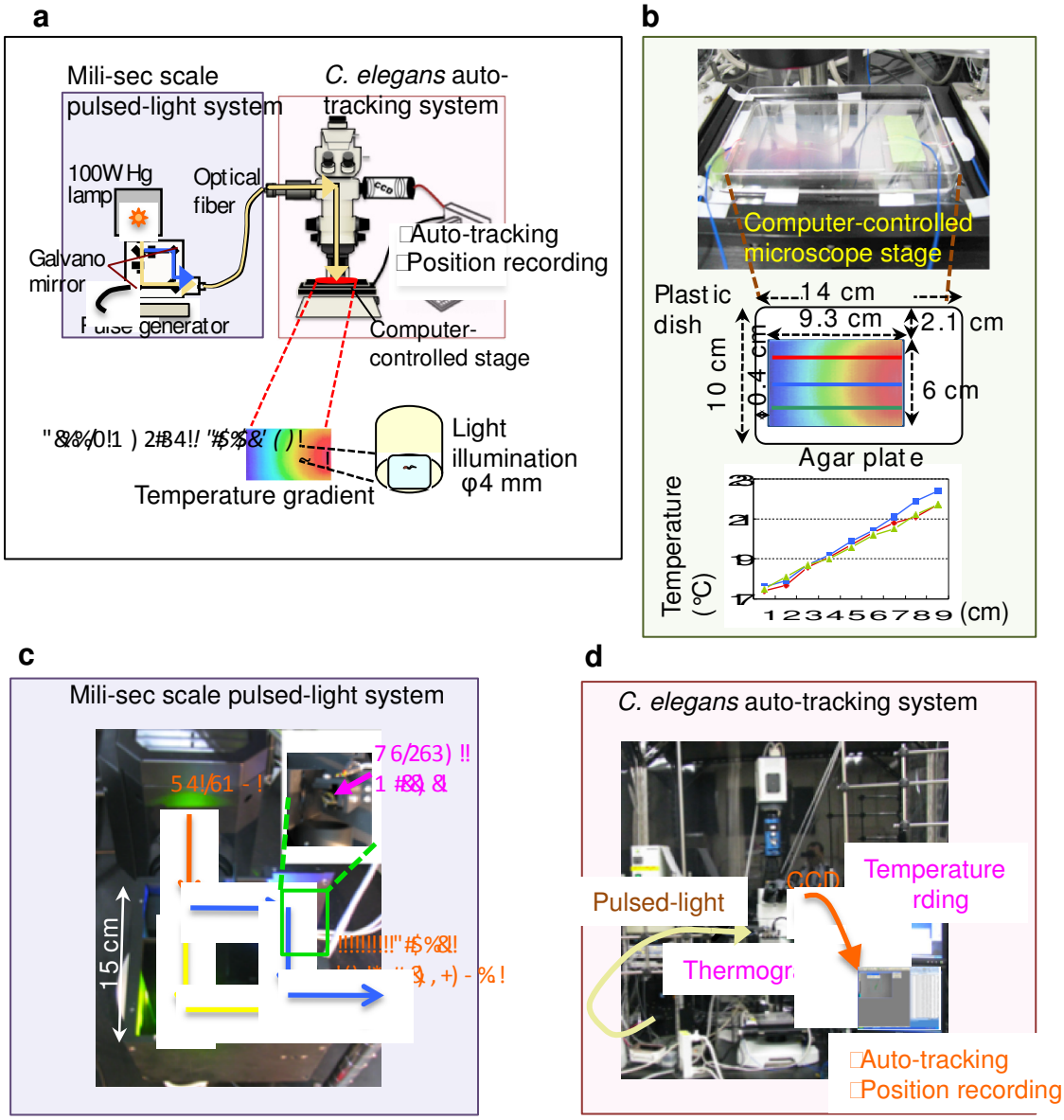

Supplementary Figure S1. Custom-made microscopic system for pulse-illuminated activation of halorhodopsin in an animal freely moving on a thermal gradient.
(**a**) A schematic diagram of optical imaging and tracking system for an animal performing thermotaxis on a thermal gradient. Thermal gradient is equipped on the computer-controlled microscope stage. In pulsed-light generation system, the light from mercury lamp (Hg lamp) was separated to yellow and blue light by dichroic mirror (Left panel). Illumination hertz and time of excitation light was controlled by galvano mirror connected with pulse-generator (Left panel). An optical fiber transmits pulsed-light to a freely moving animal through light path in microscope. (**b**) Temperature gradient on a microscope stage. 9.3 cm × 6 cm agar was placed on a plastic dish equipped on the thermal gradient stage. The temperature of the thermal gradient on agar surface was measured by both thermography and thermistor thermometer. The center of the 9.3-cm-long agar was adjusted to 20℃. A thermal gradient ranging from approximately 17.6℃ to 22.4℃ was established on the agar surface. (**c**) A Mili-sec scale pulsed-light system using galvano mirror. (**d**) *C. elegans* auto-tracking system equipping a thermal gradient on the computer-controlled microscope stage.

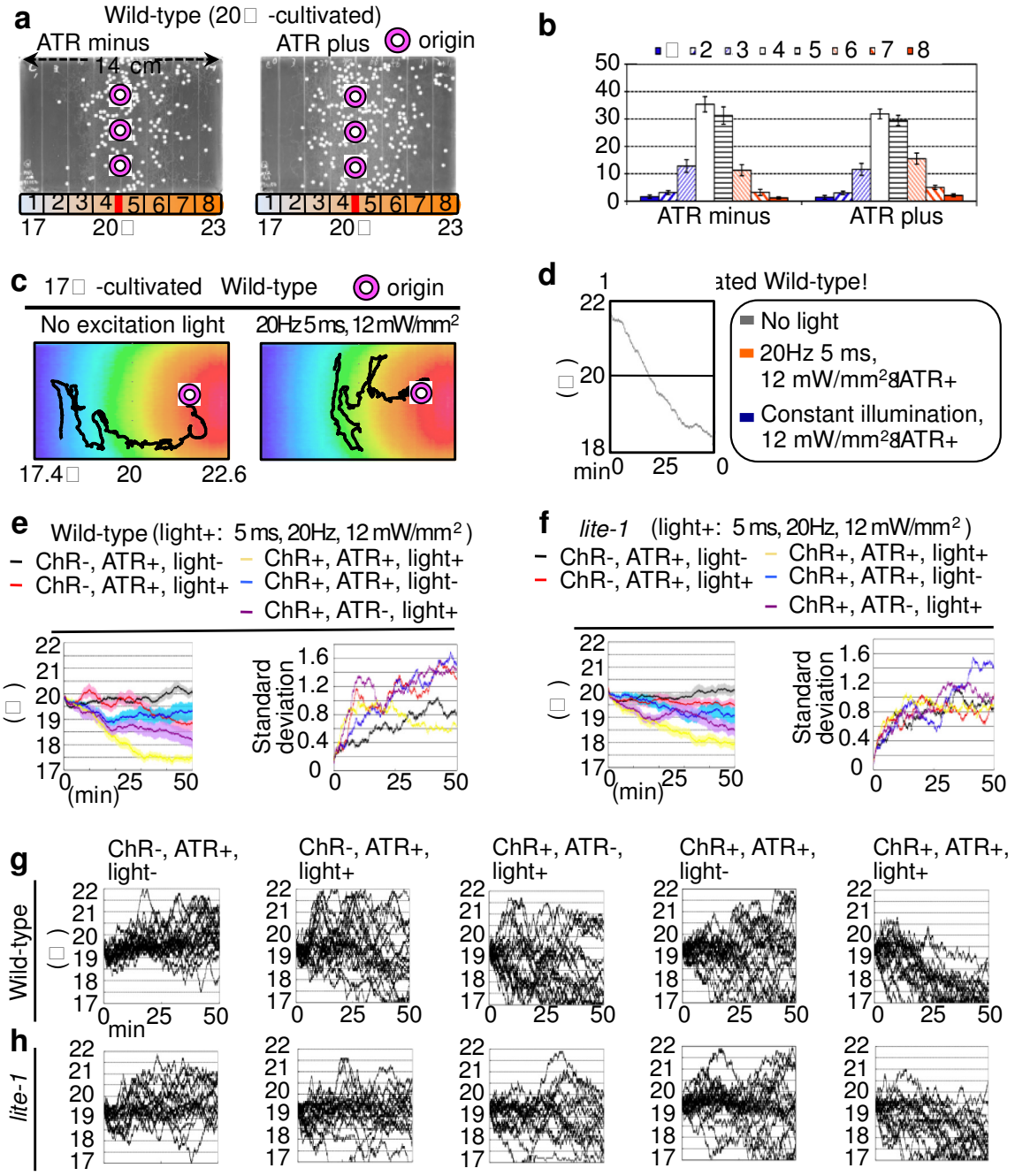

Supplementary Figure S2. Thermotaxis of animals expressing HR or ChR.

(**a**) Thermotaxis of animals cultivated with ATR. Animals cultivated at 20℃ were placed at the surface of agar with 20℃ and left for 1 hour. White dots indicate terminal positions of freely moving individual animals after 1hr test. The assay plate was divided into eight regions. (**b**) Distributions of the animals after 1hr test. Error bar indicates SEM. Average of 7 assays with ~1000 animals for each condition. (**c**) Thermotaxis of 17℃-cultivated animals expressing halorhodopsin in AFD. Representative track of an animal performing thermotaxis. (**d**) Thermotaxis of 17℃-cultivated animals. Each graph represents the average. n=17~19 for each genotype. (**e**) Thermotaxis of ChR-activated wild-type animals that were cultivated at 20℃. ChR is expressed in AFD of the animals. Error bar indicates SEM. Each graph represents the average. n=20 for each graph. (**f**) Thermotaxis of ChR-activated 20℃-cultivated *lite-1* mutants. Error bar indicates SEM. Each graph represents the average. n=20 for each graph. (**g**), (**h**) Individual traces of thermotaxis shown in e and f.

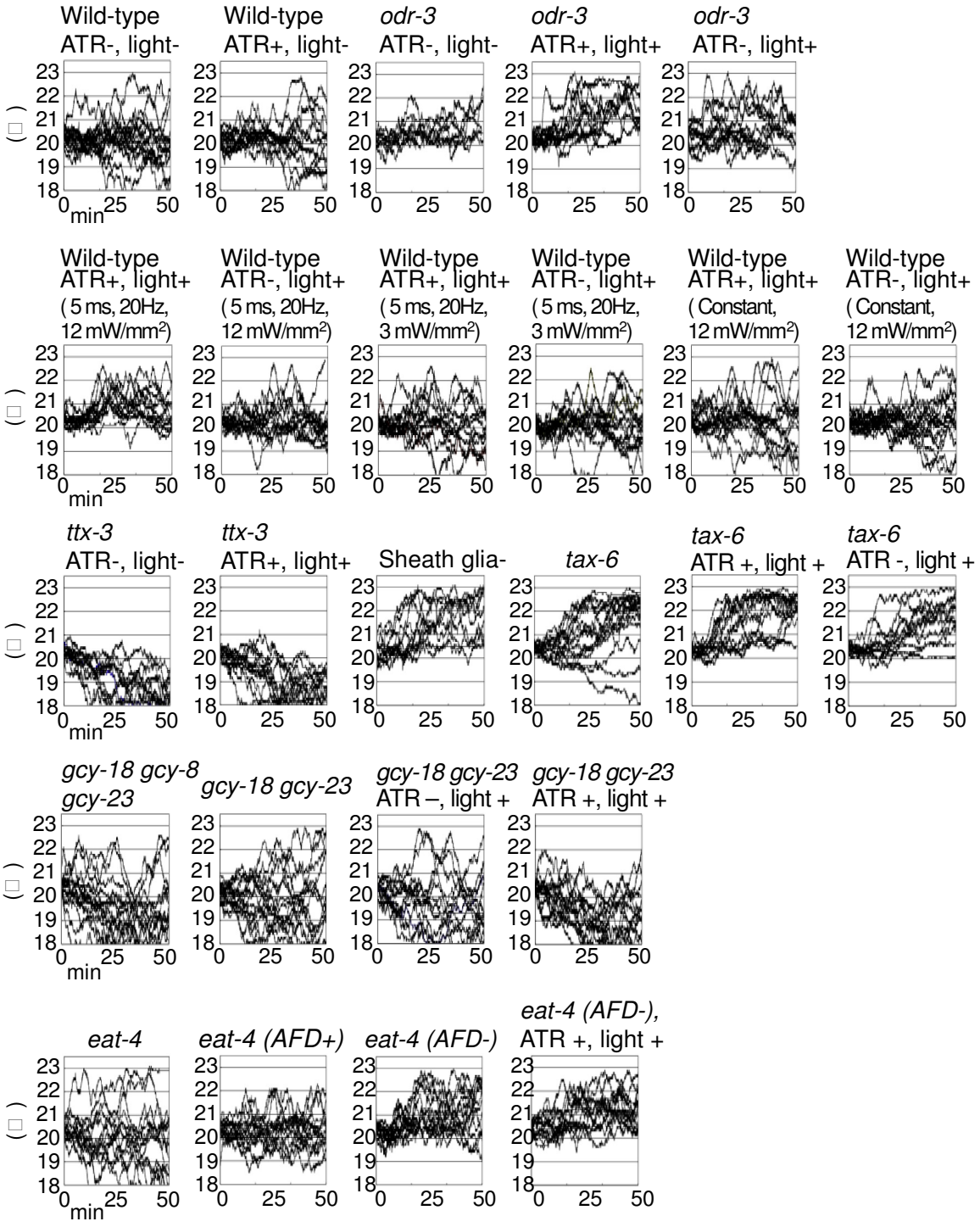

Supplementary Figure S3. Thermotactic phenotype of halorhodopsin-activated individual animals.

Individual traces of thermotactic behavior. Adult animals cultivated at 20℃ were individually placed on a 9.3 cm thermal gradient between 17.6℃ and 22.4℃, and were allowed to move freely for 50 min. n=15~19 for each genotype. Halorhodopsin is expressed specifically in AFD of the animals. The temperature of the thermal gradient was measured by thermography. Statistical data are shown in Figure 1 and 3.

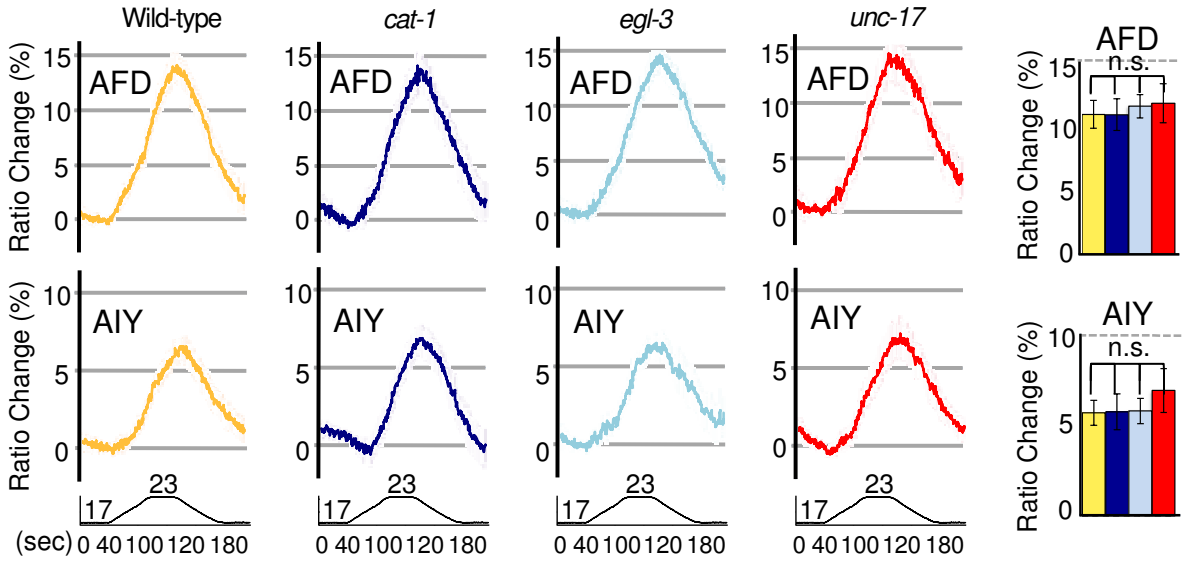

Supplementary Figure S4.
Calcium imaging in mutant animals with impairment in stimulatory neurotransmission. Calcium imaging of AFD and AIY neurons in animals subjected to warming and cooling. Temperature change with time is shown at the bottom of the graph. The *unc-17* gene encodes a synaptic vesicle acetylcholine transporter (VAChT). The *cat-1* gene encodes a synaptic vesicular monoamine transporter. The *egl-3* gene encodes a proprotein convertase processing neuropeptide. Bar graph, average ratio change during the 20 sec period from 100 to 120 sec after starting temperature change. The color key for the bar graph is the same as that for the corresponding response curve. Error bar indicates SEM. Each graph represents the average. n.s., not significant. n=17~21.

a

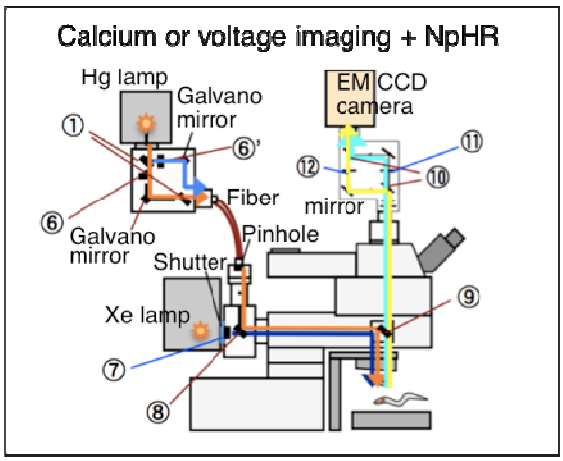

b

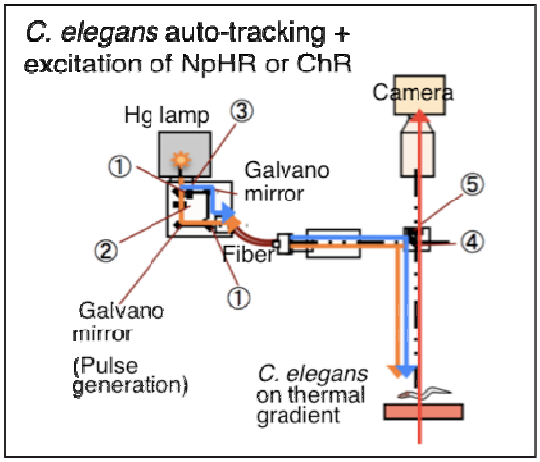

c

Approximate wave length (nm)

Number, Company, Model number	Transmission	Reflection (R) or absorption	Comment
① Olympus DM505	505≦	≦505 (R)	U-MWIB3 dichroic mirror etc.
② Olympus 25BP565	545~580	≦545, 580≦	U-MWIY2 excitator (NpHR excitation)
③ Olympus 25BP450	420~480	≦420, 480≦	U-MSWB2 excitator (ChR excitation)
④ Semrock FF677-Di01-25x36-45°Beamsplitter	677≦	≦677 (R)	Dichroic mirror for tracking, NpHR and ChR
⑤ Semrock FF01-688/31-25	657~719	≦657, 719≦	Barrier filter for tracking
⑥ Chroma HQ590/55x	540~660	≦540, 660≦	NpHR excitation
⑦ Olympus BP425-445HQ	425~445	≦425, 445≦	U-MCFPHQ excitator
⑧ Omega 610DRLP	≦530, 610≦	530~610 (R)	Combination dichroic mirror for NpHR
⑨ Olympus Custom made	450~560, 630≦	410~440, 560~630 (R)	DM for yellow cameleon and tracking
⑩ Chroma 505DCXR	505≦	≦505 (R)	CFP/YFP Beamsplitter in Dual View
⑪ Chroma D480/30m	450~505	≦450, 505≦	Dual View: barrier filter for CFP
⑫ Semrock FF01-531/22-25	509~553	≦509, 553≦	Dual View: barrier filter for YFP

d

① Olympus DM505	505≦	≦505 (R)	U-MWIB3 dichroic mirror etc.
⑥ Chroma HQ620/60	590~650	≦590, 650≦	NpHR excitation
⑥' Olympus KO/MICY FRET Excitator	440~460	≦440, 460≦	Mermaid excitation
⑦ Olympus All-reflective mirror	Non	All band	All band reflection
⑨ Olympus custom made dicroic mirror	470~585	440~470, 585~750 (R)	Dicroic mirror for mermaid and NpHR
⑩ OI-11-EM 565dcxr	565≦	≦565	Dicroic mirror
⑪ Olympus KO/MICY FRET Emitter	475~540	≦475, 540≦	Mermaid emitter for UKG
⑫ Semrock FF01-560/25-25	535~585	≦535, 610≦ (R)	Mermaid emitter for mKO*k*

Supplementary Figure S5. A schematic diagram of an optical system.

(**a**) A schematic diagram of a microscopic system for halorodopsin-activation with calcium or membrane voltage imaging. (**b**) A schematic diagram of an optical system for pulsed-activation of halorhodopsin or ChR in an animal performing thermotaxis. (**c**) Bandpass filters for experiments using halorhodopsin, ChR and yellow cameleon. (**d**) Bandpass filters for simultaneous use of mermaid and halorhodopsin. (**c**), (**d**) Each circled number corresponds to each numbered-bandpass filter represented in a, b.

Supplementary Note 1

Activation of channel rhodopsin in AFD causes cryophilic abnormality

To investigate the behavioral phenotype of the animals upon artificial activation of AFD, we employed the light-driven cation channel, channel rhodopsin (ChR2) (Supplementary Fig. S2e, g). As previously reported, illumination of blue light to channel rhodopsin rapidly activates its ion channel, allowing the influx of cations into the cell, which increases neuronal activity[37, 38]. Wild-type animals expressing ChR2 in AFD without illuminating blue light (Supplementary Fig. S2e blue line) showed a weak cryophilic phenotype. Likewise, blue light itself, without expressing ChR2 (Supplementary Fig. S2e red line), induced a weak cryophilic phenotype. This suggests that both the expression of ChR2 in AFD and blue light can disturb thermotaxis. We found that activation of ChR2 in AFD induced a stronger cryophilic abnormality (Supplementary Fig. S2e yellow line) than blue light itself. These results indicate that excitation of ChR2 causes a cryophilic abnormality, although both expression of ChR2 in AFD and blue light also affect thermotaxis.

To eliminate the side effect of blue light, we used *lite-1* mutant animals, which are defective in avoidance behavior against blue light [39,40]. The *lite-1* gene encodes a blue light receptor that is expressed in sensory neurons [39,40]. We expressed ChR2 in AFD of the *lite-1* mutant animals. The cryophilic abnormality in wild-type animals induced by blue light was partially suppressed by *lite-1* mutation (Supplementary Fig. S2f red line), although blue light still induced a weak cryophilic abnormality even in *lite-1* mutants. *lite-1* mutants expressing ChR2 in AFD without blue light showed a weak cryophilic phenotype (Fig. 2f blue line), suggesting that the expression of ChR2 impairs AFD function. We found that activation of ChR2 in AFD of *lite-1* mutant animals exhibited a stronger cryophilic abnormality (Fig. 2f yellow line). Although excitation of ChR2 in AFD induced a cryophilic abnormality (Fig. 2f yellow line), its etiology is probably complex, influenced by factors such as the additive effect of blue light, the artificial expression of ChR2 in AFD, and the excitation of ChR2.

It is important to conduct optical imaging of neuronal activity in animals when activating ChR2 in AFD to monitor the effect of ChR2-derived activation in the AFD-AIY circuit. We could not, however, perform calcium imaging with ChR2 experiments in our macroscopic systems, because the bandpass of excitation light for ChR2 overlapped with the bandpass of excitation light for the calcium indicator.

Supplementary References

37 Nagel, G. *et al.* Channelrhodopsin-2, a directly light-gated cation-selective membrane channel. *Proc Natl Acad Sci U S A* **100**, 13940-13945 (2003).

38 Zhang, F. *et al.* Multimodal fast optical interrogation of neural circuitry. *Nature* **446**, 633-639 (2007).

39 Edwards, S. L. *et al.* A novel molecular solution for ultraviolet light detection in Caenorhabditis elegans. *PLoS biology* **6**, e198 (2008).

40 Liu, J. *et al.* C. elegans phototransduction requires a G protein-dependent cGMP pathway and a taste receptor homolog. *Nature neuroscience* **13**, 715-712 (2010).